International Journal of Transportation Science and Technology xxx (xxxx) xxx

Contents lists available at ScienceDirect

International Journal of Transportation Science and Technology

journal homepage: www.elsevier.com/locate/ijtst

Research Paper

Vehicle carbon emission estimation for urban traffic based on sparse trajectory data

Wanjing Ma, Yuhan Liu, Philip Kofi Alimo, Ling Wang *

The Key Laboratory of Road and Traffic Engineering of the Ministry of Education, Tongji University, 4800 Cao'an Road, Shanghai 201804, PR China

ARTICLE INFO

Article history:
Received 9 March 2023
Received in revised form 30 October 2023
Accepted 31 January 2024
Available online xxxx

Keywords:
Carbon emission
Second-by-second data
Acceleration distribution
Sparse trajectory data
Trajectory reconstruction

ABSTRACT

Sparse trajectory data with non-second-by-second sampling intervals are common. However, most carbon emission estimation models for vehicles require second-by-second inputs. Additionally, some models ignore the emission generation principle, and some have complicated inputs. To address these limitations, this study proposes a vehicle carbon emission estimation method for urban traffic, based on sparse trajectory data. First, a trajectory reconstruction method based on interpolation of acceleration distribution is proposed. The results showed that the reconstructed trajectory was close to the real trajectory, and the accuracy was 2–17% higher than that of other methods. Second, a carbon emission estimation model that considers both the emission generation principle and feasibility is proposed. The model with a goodness-of-fit of 0.887 had the best performance compared to the other models. The emission estimation results of the reconstructed sparse trajectories showed that the precision improved significantly for data with different frequencies compared to that of other reconstruction methods, e.g., 9% higher at a 30 s sampling interval.

1. Introduction

Carbon emissions have rapidly increased over the past 70 years and remain a major contributor to global climate change. According to the International Energy Agency, carbon emissions from the transportation sector account for approximately 25% of the total emissions, and have become the second largest source of carbon emissions (International Energy Agency, 2021). Emissions from the transportation sector increase faster than those from other economic sectors (Sun et al., 2022, Raymand et al., 2021), and among all transportation sectors, on-road vehicle emissions are an important source of emissions (Mingolla and Lu, 2021). Therefore, carbon emissions from vehicle exhaust have garnered increasing attention in recent years (Di Battista and Cipollone, 2016, He et al., 2018). Quantifying or estimating carbon emissions is vital for developing better carbon mitigation strategies and policies (Grote et al., 2018).

With the widespread use of GPS navigation and positioning terminals, massive trajectory data can easily be obtained, which facilitates the estimation of vehicular emissions. However, because of the high cost of second-by-second (SBS) trajectory data acquisition, storage, and communication, common GPS devices in vehicles generally upload data at low frequen-

Peer review under responsibility of Tongji University and Tongji University Press.
* Corresponding author.
E-mail addresses: mawanjing@tongji.edu.cn (W. Ma), yuhanliu@tongji.edu.cn (Y. Liu), alimokofi2020@tongji.edu.cn (P.K. Alimo), wang_ling@tongji.edu.cn (L. Wang).

https://doi.org/10.1016/j.ijtst.2024.01.010
2046-0430/

cies, e.g., 10 s and 30 s (Chen et al., 2021, Quddus and Washington, 2015). This forms a sparse trajectory data record that poses challenges in estimating emissions because the inputs of most emission estimation models for estimating individual vehicle emissions generally require SBS vehicle operating data (Nam and Giannelli, 2005, Shafabakhsh et al., 2018, Zhang and Ioannou, 2016). To estimate the emission based on sparse trajectory data, some researchers attempted to reconstruct the trajectory, obtained the estimated SBS trajectory points (Sun et al., 2015, Hao et al., 2014), and finally calculated the emissions based on the reconstructed SBS trajectory points. The most important foundation for the above method is trajectory reconstruction, which directly affects the estimation precision. For different traffic parameter estimation or specific traffic scenarios, there are various reconstruction or indirect derivation methods based on sparse trajectory data (Chen et al., 2022). These methods can be divided into three main categories, which include smooth interpolation methods (Venthuruthiyil and Chunchu, 2018), mixed interpolation methods combining with a priori traffic flow empirical value (Chen et al., 2018), and models based on microscopic traffic flow and multi-source heterogeneous data (Xie et al., 2018). The objectives of trajectory reconstruction can be divided into travel time estimation (Li et al., 2018, Qin et al., 2023) and traffic status identification (Ma and Zhu, 2021, Wang et al., 2019). However, due to different objectives, the trajectory reconstruction methods are difficult to migrate directly. To enhance the accuracy of emission estimation, the variation trend of velocity or acceleration per second is crucial. For estimating travel time, improving the accuracy of travel time estimation of unit trajectory segments is more critical than the accuracy of the instantaneous acceleration estimation. Most previous studies used simple interpolation methods for vehicle carbon emission estimation. For example, they assumed that the acceleration/deceleration values were constant (Yang et al., 2011) or varied linearly (Shan et al., 2018, Hao et al., 2016), and used linear (Liu et al., 2013) or cubic spline interpolation methods (Chang et al., 2012, Li et al., 2019) to fill the trajectory data. The trajectories reconstructed by these methods are usually stable and cannot capture changes in the vehicle status. In particular, for urban traffic flow, for example, vehicles on arterials and collectors, the frequency and range of acceleration and deceleration behaviors are much higher than those on expressways. The estimated acceleration was relatively stable based on simple interpolation methods, resulting in a significant underestimation of the emissions. Additionally, some studies proposed other methods such as reconstructing trajectory based on sequence decision to estimate emissions over a long distance or a long period (Wang et al., 2017), a traffic energy consumption model based on the macro–micro data (Shang et al., 2023), and carrying out operating condition measurement experiments for specific vehicle types in particular areas (Weng et al., 2017). There are also researches on estimating average speed between two consecutive timestamps by map matching algorithm to approximate the instantaneous speed (Liu et al., 2019) or reconstructing an individual trip chain through road average speed and speed correction factors (Liu et al., 2023). Most of these aforementioned studies have limitations in the scope and conditions of application.

Another key issue in estimating carbon emissions based on sparse trajectory data is the determination of the estimation model. The United States and some countries in Europe were the first to realize the importance of quantifying emissions, and many studies have been conducted on establishing vehicle emission estimation models since the 1950s. In recent years, many typical models have been improved and widely used worldwide, such as MOBILE (EPA, 2003), MOVES (U.S. Environmental Protection Agency, 2021), COPERT (Ntziachristos et al., 2009), EMFAC (EMFAC, 2006), and IVE (Davis et al., 2005). Most of these models are aimed at estimating large-scale emission inventories of road networks, rather than individual vehicles. The shortcomings of models that can estimate micro-level emissions, i.e., individual vehicle emissions, are as follows. First, some of them were based on data from limited driving cycles, which were different from the real driving situations on roads (Chindamo and Gadola, 2018). Second, the inputs of some models ignored the emission generation principle and were only based on speed and acceleration, which would result in poor interpretability of the model (Rakha et al., 2004). Some other models have specifically been developed for estimating micro-level emissions that consider the physical principle of motor vehicle emission generation, for example, VERSIT+ (Smit et al., 2007) and CMEM (Scora and Barth, 2006). However, such models generally have complicated inputs, and the internal engine operating data of each vehicle cannot be obtained easily. To some extent, using trajectory data has a higher value than using instantaneous vehicle engine operating data because trajectory data are easier to collect in practice. Most of the literatures on vehicle emission estimation in recent years are still based on these aforementioned models, such as using the COPERT model to estimate emissions from urban roads or highways (Lejri et al., 2018), estimating emissions of both individual vehicle and a network area based on COPERT and GPS big data (Kan et al., 2018), simulating trajectory data with SUMO and calculating mixed traffic flow emissions with VT-Micro model (Zhao et al., 2022), estimating road emissions based on data from traffic radars and video-cameras and MOVES (Xu et al., 2018), and some application studies of CMEM for estimating vehicle emissions (Pathak et al., 2016; Turkensteen, 2017).

Based on the above limitations, this study aims to achieve the following objectives:

(1) To propose a reconstruction method for sparse trajectory data based on interpolation of acceleration distribution. The data of each point between the two given trajectory points are expected to be estimated as accurately as possible, which is the foundation of emission estimation.
(2) To establish a vehicle carbon emission estimation model based on SBS trajectory data, considering both the emission generation principle and feasibility.

The remainder of this paper is organized as follows. The second section presents the data-preparation process. The third section describes the reconstruction method for sparse trajectory data based on interpolation of acceleration distribution

and the estimation model for vehicle carbon emissions. The fourth section presents the numerical results through a case study. Finally, the discussion and concluding remarks are presented in the fifth section.

2. Data preparation

2.1. Data collection

A large amount of SBS vehicle trajectory and carbon emission data were collected between February and July 2022 in several cities in northern, central, and southern China. As the research object of this study is urban traffic flow, the data of vehicles driving on arterials and collectors were first filtered by road network matching technology based on the position information. Collecting field data from roads has a significant advantage over collecting data from a few driving cycles. This is because it is difficult to cover the entire vehicle's operational regime with only a few driving cycles. The vehicles in this experiment were 13 light-duty vehicles, and the duration of each vehicle was more than 90 min. The total data collection time and total distance were 24.5 h and 834 km, respectively. The data collection information is shown in Table 1.

To collect the data, the on-board diagnostics (OBD) device was connected to the OBD interface of the vehicle to export all vehicle-running data files. The intelligent terminal OBD device simultaneously collected the SBS longitude, latitude, speed, and other trajectory data of the vehicle, as well as the instantaneous fuel consumption. Carbon emissions were directly converted from the fuel consumption using the chemical equation of fuel combustion. By connecting to the vehicle OBD interface directly, the most precise vehicle operation data were obtained, excluding external factors. Additionally, acceleration data were not directly collected, but were calculated using the instantaneous speed.

2.2. Cutting and classifying the trajectory pieces

Trajectory reconstruction is essential for estimating the emissions based on sparse trajectory data. The objective is to obtain the acceleration of each point in the sparse trajectory, given the starting and ending trajectory points. Assuming that there is no significant difference between the driving patterns for SBS and sparse trajectory data, the acceleration distribution of the SBS trajectory data would be similar to that of the sparse trajectory. Thus, the acceleration distribution estimated based on the SBS trajectory data can support sparse trajectory reconstruction. Given that the sampling frequency of the sparse trajectory is r s, the SBS trajectory is cut into different pieces at the same interval (r s). Subsequently, because similar starting and ending driving characteristics, such as the speed value and range, might have the same acceleration distribution, the pieces are classified into bins. The detailed steps are as follows.

(1) The trajectory piece sequence was cut. The SBS trajectory data were cut at the r s interval. For example, if r is equal to three, then the 1-2-3-4 s and 4-5-6-7 s data form a trajectory piece, respectively.
(2) Trajectory pieces were then classified. The difference between the ending speed v_{r+1} and the starting speed v_1 (i.e., $v_{r+1} - v_1$) of the piece forms the basis for division. First, pick out all trajectory pieces wherein the vehicle runs at a speed standard deviation of less than 1.5 m/s. Second, the speed of each piece was calculated to obtain the upper-bound $v_{r,\max}$ and lower-bound $v_{r,\min}$. Third, all the trajectory pieces were divided based on $v_{r,\max}$ and $v_{r,\min}$. If the result is $v_{r+1} - v_1 \geqslant v_{r,\max}$, the piece is defined to be in a state of unsteady acceleration (UA). If the result is $v_{r+1} - v_1 \leqslant v_{r,\min}$, the piece is defined to be in a state of unsteady deceleration (UD). If the result is $v_{r,\min} < v_{r+1} - v_1 < v_{r,\max}$, the piece is defined to be in a state of relative steady speed (SS).

Table 1
Data collection information.

Vehicle ID	Engine Displacement (L)	Vehicle Curb Weight (kg)	Experimental Date	Valid Duration (min)	Travel Range (km)	Location
1	2.0	1456	2022/2/12	100	62	Shanxi province
2	1.6	1174	2022/3/22	115	65	Shanghai
3	1.6	1581	2022/6/29	99	61	Liaoning province
4	1.5	1276	2022/6/29	96	62	Liaoning province
5	1.5	1195	2022/6/30	92	52	Liaoning province
6	1.6	1343	2022/6/30	99	44	Liaoning province
7	1.5	1335	2022/6/30	120	76	Guangxi province
8	1.4	1445	2022/7/1	122	69	Liaoning province
9	2.0	1540	2022/7/1	111	69	Liaoning province
10	1.5	1590	2022/7/2	102	56	Liaoning province
11	1.5	1315	2022/7/2	124	59	Liaoning province
12	1.6	1444	2022/7/3	158	82	Liaoning province
13	1.5	1519	2022/7/3	136	77	Liaoning province

(3) Trajectory pieces were further divided into bins. For the SS state, binning is based on the average speed of a piece with a step length of s km/h. The acceleration distributions under different average speed ranges will differ. For example, when the average speed is low, the vehicle has a high probability of idling, leading to a higher zero acceleration ratio. As the average speed increases, the frequency of the acceleration and deceleration behaviors is probably higher. Thus, the acceleration distribution is more dispersed. The basis of binning for UA and UD is v_1 and $v_{r+1} - v_1$. $v_{r+1} - v_1$ reflects the pattern of speed fluctuation, which directly determines the acceleration distribution, and the starting speed v_1 affects the range of acceleration and deceleration. Thus, both v_1 and $v_{r+1} - v_1$ constitute to the basis of the binning division.

(4) The Kolmogorov-Smirnov (K-S) test was conducted to test the significance of the difference in the acceleration distribution between different bins. After the binning process, the significance of the difference between every pair of bins needs to be checked. This step is conducted to ascertain whether it is reasonable to calculate the distribution function separately or whether the two bins should be combined when no difference is observed. For SS, UA, and UD, pairwise testing was conducted between every two bins. The null hypothesis of the K-S test H_0 is as follows: "There is no significant difference in the acceleration distribution between the two bins." The distribution functions were set as $F_i(x)$ and $F_j(x)$, respectively. The statistic of the test is then expressed in **Eq. (1)**:

$$D_{i,j} = \max \left| F_i(x) - F_j(x) \right| \tag{1}$$

The p-value is calculated. If $p < 0.05$, the H_0 was rejected. Otherwise, the two bins were merged.

$$p = P\left\{ D_{i,j} > c(\alpha) \cdot \sqrt{\frac{m+n}{m \cdot n}} \right\} \tag{2}$$

where $c(\alpha)$ is a constant corresponding to the confidence level α. m and n represent the sample sizes of bins i and j, respectively.

2.3. Variable description for the estimation model

The carbon emission estimation model was established based on the collected SBS trajectory data. First, the data were cleaned to reduce the noise of the raw data, including consistency checks, invalid data deletion, and rectification of missing values to ensure model quality. There were 80,020 valid pieces of data after cleaning. Sensitivity analysis was conducted on the data sample size, which confirmed that significant variables and coefficients remained stable when the data sample size reached 50,000. The total sample size exceeded the threshold.

Second, the independent and dependent variables were determined. The vehicle specific power (VSP) is the ratio of the rated power of the vehicle engine to the maximum design total mass. Many related studies and existing estimation models have demonstrated a direct connection between the VSP and emission estimation (Song and Yu, 2009, Zhang et al., 2019, Song and Yu, 2011). VSP is a comprehensive indicator for evaluating the power performance of a vehicle, which reflects the emission generation principle and can be indirectly calculated using common traffic parameters (Jimenez-Palacios, 1998). This helps improve the precision and interpretability of the input parameters of the emission model. The formula is as follows:

$$VSP = v(1.1 \cdot a + 0.132) + 0.000302\, v^3 \tag{3}$$

where v is the instantaneous speed (m/s) and a is the instantaneous acceleration (m/s^2), which can be positive, 0, or negative. Therefore, for the proposed estimation model in this study, the instantaneous speed and acceleration collected directly from the trajectory data and the indirectly calculated VSP are the independent variables. The instantaneous carbon emission rate is the dependent variable.

Third, because large masses of raw data are discrete, the direct fitting regression effect is presumed to be poor. Therefore, the raw data can be divided into several bins at small intervals according to the speed and acceleration parameters. Specifically, a binning procedure is created to reduce the number of raw data points. The emissions of all vehicles in the same speed/acceleration bin are averaged to generate a single average emission estimate. The division method is determined based on the value range and sample size of the data. The sample size within each bin should not be too small or significantly different. In this study, the speed bins included speeds ranging from 0 to 80 km/h at increments of 2 km/h, while acceleration bins included accelerations ranging from −3.3 to 3.3 m/s^2 at increments of 0.3 m/s^2.

3. Methodology

As shown in Fig. 1**,** there are two essential parts of estimating vehicle carbon emissions based on sparse trajectory data. These include the trajectory reconstruction and estimation regression models.

3.1. Sparse trajectory reconstruction method

This reconstruction method uses the acceleration distribution as the core guideline because general simple interpolation methods ignored the kinematic principles of the vehicle. The constructed stable trajectory cannot reflect the stochastic characteristics of the change in vehicle speed, thereby underestimating the emissions. Acceleration is the key influencing factor in emission estimation, which determines the trend of speed variation and is also an independent variable of the VSP parameter. VSP is closely related to emission, and it is sensitive to the variation of acceleration. Therefore, directly estimating acceleration not only helps to reproduce the real trajectory with stochastic acceleration and deceleration behaviors, but also affects the precision of emission estimation.

3.1.1. Establishing the acceleration distribution model

The acceleration distribution reflects the probability of the occurrence of different acceleration values. Therefore, the probability density function $f(x)$ was used to describe the acceleration distribution under different operating conditions. The integration of $f(x)$ in the interval (a, b) is the probability of occurrence of the random variable X in this interval.

$$P\{a < X < b\} = \int_a^b f(x)dx \tag{4}$$

The 11 comprehensive and most commonly used distribution functions were selected to fit the acceleration data contained in each bin of SS, UA, and UD to the probability density functions. The probability density functions included the norm, expectation, Pareto, Weibull, T, extreme, gamma, log-norm, beta, uniform, and log-gamma functions. The root mean square error (RMSE) and goodness-of-fit (R^2) were used to evaluate the fitting effect. The RMSE was calculated using **Eq. (5)**, which reflects the degree of the fit. The smaller the RMSE, the better is the fitting result. R^2 was calculated as shown in **Eq. (6)**. The closer the R^2 value to 1, the better is the fitting result.

$$RMSE = \sqrt{\frac{1}{m}\sum_{i=1}^{m}(y_i - \hat{y}_i)^2} \tag{5}$$

$$R^2 = \frac{ESS}{TSS} = \frac{\sum_{i=1}^{n}(\hat{y}_i - \bar{y})^2}{\sum_{i=1}^{n}(y_i - \bar{y})^2} \tag{6}$$

The distribution function with the best fit in each bin was selected as the final acceleration distribution function to estimate the acceleration of each point in the sparse trajectory.

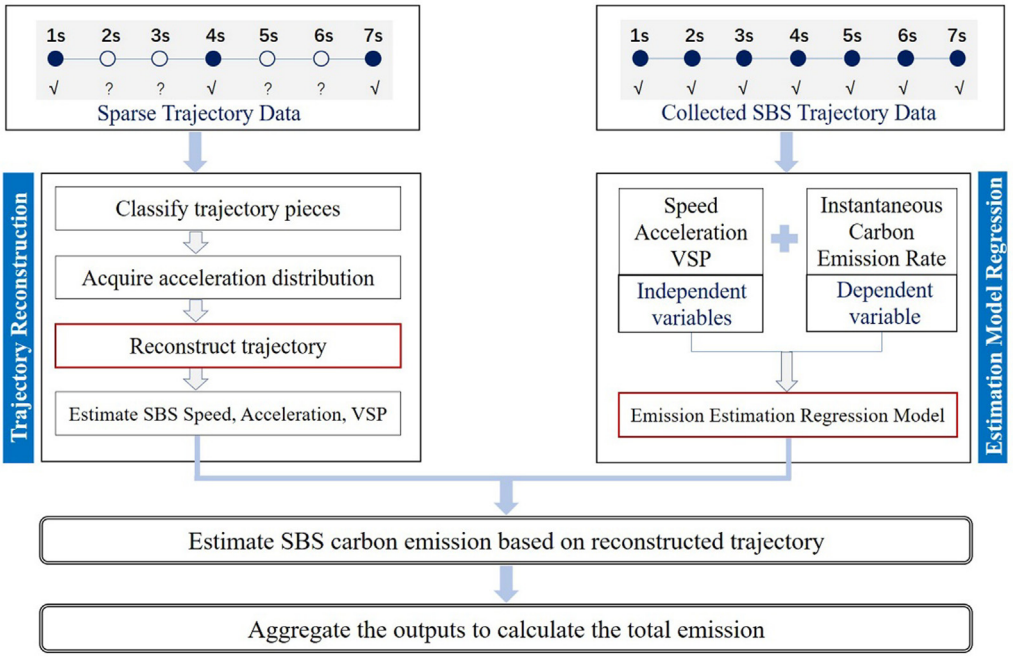

Fig. 1. The two essential parts of the emission estimation method.

3.1.2. Reconstructing the sparse trajectory

For the entire sparse trajectory sequence containing N trajectory pieces with a sampling interval r s, the speed at the sparse point is known for any trajectory piece n ($1 \leqslant n \leqslant N$). The time-series number set of the trajectory sequence with known speed is $\{1, r+1, 2r+1, ..., nr+1\}$, and the known speed set is $\{v_1, v_{r+1}, v_{2r+1}, ..., v_{nr+1}\}$. According to the established acceleration distribution model, the acceleration can be estimated at each point in the entire sparse trajectory sequence. This process is illustrated in Fig. 2.

The specific steps are as follows:

(1) The trajectory pieces were classified.
   a. *Classifying each trajectory piece into SS, UA, and UD.* For piece n, the difference between the ending speed v_{nr+1} and the starting speed $v_{(n-1)r+1}$ (i.e., $v_{nr+1} - v_{(n-1)r+1}$, ($1 \leqslant n \leqslant N$)) was calculated. If the result is $v_{r,\min} < v_{nr+1} - v_{(n-1)r+1} < v_{r,\max}$, the piece is in the SS state. If the result is $v_{nr+1} - v_{(n-1)r+1} \geqslant v_{r,\max}$, the piece is in the UA state. If the result is $v_{nr+1} - v_{(n-1)r+1} \leqslant v_{r,\min}$, the piece is in the UD state.
   b. *Dividing the pieces into bins.* Pieces in the SS state can be divided into corresponding bins based on the average speed $\frac{v_{nr+1}+v_{(n-1)r+1}}{2}$. Pieces in the UA and UD states can be divided into corresponding bins based on $v_{(n-1)r+1}$ and $v_{nr+1} - v_{(n-1)r+1}$.
(2) The trajectory data were estimated.
   a. *Acquiring acceleration distribution.* Each piece was identified as belonging to a bin and the established acceleration distribution model was acquired.
   b. *Estimating acceleration at each point.* Acceleration was estimated at each point using the acceleration distribution model.
   c. *Calculating the speed at each point.* Based on the acceleration data and the known speed at the starting point, the speed was calculated point by point.
(3) The constraints were verified.

The estimated acceleration and speed were validated to ensure that they conformed to the following constraints:

   a. *The validity of speed.* The speed at all points of v_i, $((n-1)r+1 < i \leqslant nr+1)$, except the starting point, was calculated from the acceleration; thus, there was a possibility of error. Therefore, speed v_i must satisfy the following constraint:

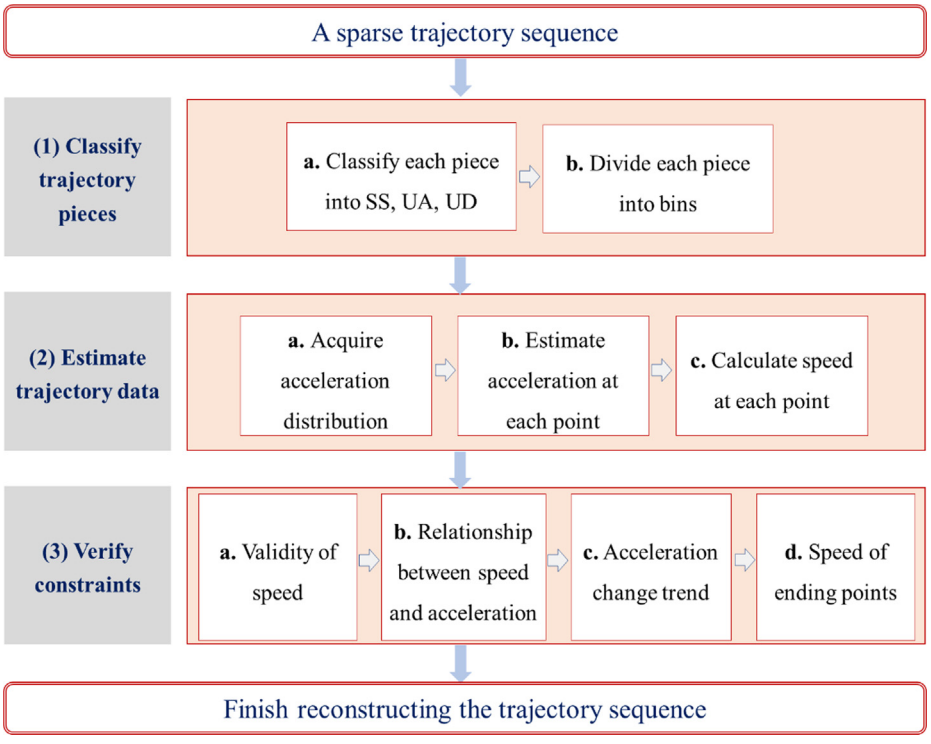

Fig. 2. The process of reconstructing trajectory.

$$v_i \in [0, V_{\max}] \tag{7}$$

where $V_{\max}$ is the speed limit on the roads.

b. *Relationship between speed and acceleration.* The acceleration fluctuation range at different instantaneous speeds is inconsistent. Therefore, the collected data were analyzed to determine the relationships between the maximum acceleration and instantaneous speed, and the minimum deceleration and instantaneous speed. Drivers tend to adjust their speed significantly to achieve the desired speed at a lower speed; thus, the acceleration tends to fluctuate more. However, at a higher speed, the driver has already achieved the desired speed; therefore, the fluctuation range is smaller for the sake of comfort. The results based on the large amount of collected trajectory data were as follows. R^2 values were 0.92 and 0.90 for **Eq. (8)** and **Eq. (9)**, respectively.

$$a_{v,\max} = -0.5422 \ln(v) + 3.33 \tag{8}$$

$$a_{v,\min} = 0.5422 \ln(v) - 3.33 \tag{9}$$

where $a_{v,\max}$ and $a_{v,\min}$ represent the maximum acceleration and minimum deceleration at v, respectively, and the unit of v is km/h.

According to $a_{v,\min}$ and $a_{v,\max}$, there is a constraint for a_i when the speed is v_i:

$$a_i \in \left[a_{v_i,\min}, a_{v_i,\max}\right], \quad ((n-1)r + 1 \leqslant i \leqslant nr + 1) \tag{10}$$

c. *Change trends of acceleration/deceleration.* This constraint is used to avoid the non-conformity of the estimated acceleration/deceleration trend of consecutive points to reality. Using the collected data, the pattern of the difference between the accelerations at intervals of 0, 1, and 2 s was calculated and analyzed. The results are as follows:

$$a_{i+1} - a_i \in [-2.22, +2.22] \tag{11}$$

$$a_{i+2} - a_i \in [-2.78, +2.78] \tag{12}$$

$$a_{i+3} - a_i \in [-3.89, +3.33] \tag{13}$$

d. *Speed of ending points.* At the end of each piece, the true ending speed v_{nr+1}^{true} was known, and the estimated ending speed v_{nr+1} was calculated based on the true starting speed and acceleration at each point. The threshold of the difference was assumed to be V_{thre}. If the result is $\left|v_{nr+1} - v_{nr+1}^{true}\right| \leqslant V_{thre}$, the estimated value is accepted; otherwise, the test is considered to have failed.

(4) All the aforementioned tests and constraints must be simultaneously satisfied to obtain a valid trajectory reconstruction. Otherwise, the acceleration is estimated again point by point. If one of the above constraints is still not satisfied after several repetitions, e.g., after 1,000 repetitions, a randomly selected piece from the known trajectory pieces is used.

3.2. SBS carbon emission estimation model

A regression model for estimating vehicle emissions was established based on the collected SBS trajectory data. Regression models, such as multiple linear regression, curve estimation, and polynomial regression, can be used to establish the relationship between the speed, acceleration, VSP, and carbon emission rate. Specifically, basic linear regression is the simplest form of regression when the independent variables are multivariate, and this method works well sometimes. Considering that VSP can be indirectly calculated from speed and acceleration and is closely related to the emission, the curve estimation (including linear, quadratic, and cubic terms) using only VSP is also appropriate. Additionally, multivariate polynomial regression can handle considerable nonlinear problems and plays an important role in regression analysis because any function can be approximated using a polynomial.

As the dependent variable carbon emission rate must be positive, it is more reasonable to consider the logarithmic form of the carbon emission rate when fitting. The forms of the basic linear regression and curve estimation are as follows:

$$\ln ER = \beta_0 + \beta_1 \times v + \beta_2 \times a + \beta_3 \times VSP \tag{14}$$

$$\ln ER = \beta_0 + \beta_1 \times VSP \tag{15}$$

$$\ln ER = \beta_0 + \beta_1 \times VSP + \beta_2 \times VSP^2 \tag{16}$$

$$\ln ER = \beta_0 + \beta_1 \times VSP + \beta_2 \times VSP^2 + \beta_3 \times VSP^3 \tag{17}$$

where, ER is the instantaneous carbon emission rate (g/s). β_0,β_1,β_2, and β_3 represent regression model coefficients.

VT-Micro, a typical statistical regression emission estimation model, is a polynomial regression model for speed and acceleration that does not consider VSP as an independent variable, and its regression form is expressed in **Eq. (18)**:

$$\ln ER = \begin{cases} \sum_{i=0}^{3}\sum_{j=0}^{3}\left(L_{i,j} \times v^i \times a^j\right) & for \quad a \geqslant 0 \\ \sum_{i=0}^{3}\sum_{j=0}^{3}\left(M_{i,j} \times v^i \times a^j\right) & for \quad a < 0 \end{cases} \tag{18}$$

where $L_{i,j}$ and $M_{i,j}$ represent the regression model coefficients at "speed to the power of i" and "acceleration to the power of j." v is the instantaneous vehicle speed (km/h) and a is the instantaneous vehicle acceleration (km/h/s). A piecewise function is developed for positive and negative accelerations because the vehicle exerts power during positive acceleration, whereas it does not exert power in the negative acceleration range.

However, according to the working principle of motor vehicles, in addition to the acceleration and deceleration states, the engine condition in the idle mode is also significantly different. A better method should be considered to divide the vehicle operation into three states: deceleration, acceleration, and idling. The idling state refers to $v < 1.6km/h$, whereas $v \geqslant 1.6km/h$ *and* $a \geqslant 0$ and $v \geqslant 1.6km/h$ *and* $a < 0$ are the acceleration and deceleration states, respectively. In this study, a polynomial regression model was established, as expressed in **Eq. (19)**:

$$\ln ER = \sum_{i=0}^{3}\sum_{j=0}^{3}(L_{i,j} \times v^i \times a^j) + \sum_{l=0}^{1}\sum_{m=0}^{1}\sum_{n=1}^{3}(M_{l,m,n} \times v^l \times a^m \times VSP^n) \tag{19}$$

where $L_{i,j}$ represent the regression model coefficients at "speed to the power of i" and "acceleration to the power of j," and $M_{l,m,n}$ represents the regression model coefficients at "speed to the power of l," "acceleration to the power of m," and "VSP to the power of n." Each segment of the piecewise function requires its fitting process. As the equation contains a large number of variables, the significant variables can be filtered into the final regression model using the forward method (Härdle and Simar, 2019).

To conduct different fitting processes, the choice of the regression model, necessity of the piecewise function, establishment of the piecewise function, and design of the binning rules for raw data were considered. The index used to determine the fitting effect was the goodness-of-fit (R^2). The larger the R^2 value, the better is the fit. Simultaneously, regression model proposed in this study was compared with commonly used models to verify whether its effectiveness.

4. Results

4.1. Results of the trajectory reconstruction method

The trajectory reconstruction was based on a real trajectory sequence of 120 s. The sampling intervals were 5, 15, and 30 s. The interpolation method of acceleration distribution (Method I), linear interpolation (Method II), and cubic spline interpolation (Method III) were conducted. The results are shown in Fig. 3. If the differences between the estimated and true values of speed are within 5, 10, and 20% of the true values at sampling intervals of 5, 15, and 30 s, respectively, the trajectory point is considered to be estimated relatively accurately. In this study, the proportion of approximately accurate estimated points among all trajectory points of the sequence is called the accuracy of the trajectory reconstruction. The accuracy of the trajectory reconstruction results is shown in Fig. 4.

Fig. 3 shows that the trajectories reconstructed by the linear interpolation and cubic spline interpolation methods were relatively stable. The trajectory points were directly connected by smooth lines. When the sampling frequency was high (5 s), the trajectories reconstructed by the three methods differed less from the real trajectories from the perspective of intuitive observation. This is because there were sufficient known points that can be used to constrain the trends of the reconstructed trajectories. The accuracy of the trajectory reconstruction results of Method I was 2.5 and 5.8% higher than those of Methods II and III, respectively. When the sampling frequency was slightly lower (15 s), the trajectories reconstructed by the other two methods for unknown points were not in line with the real situation. The trajectory reconstructed using the method proposed in this study can satisfactorily reproduce the real trajectory. The accuracy of the trajectory reconstruction of Method I was 62.8%, which was higher than those of the other two methods. When the sampling frequency was very low (30 s), the other two methods almost completely lost the function of trajectory reconstruction. Although the method proposed in this study cannot precisely reproduce the acceleration and deceleration over a period of 30 s, it can still partly reflect the stochastic behaviors of acceleration and deceleration. The accuracy of the trajectory reconstruction results of Method I was 17.3% and 7.4% higher than those of Methods II and III, respectively. Fig. 4 shows that the accuracy of the trajectory reconstruction decreases as the sampling interval increases because the sparser the sampling interval, the more difficult it is to accurately estimate each point.

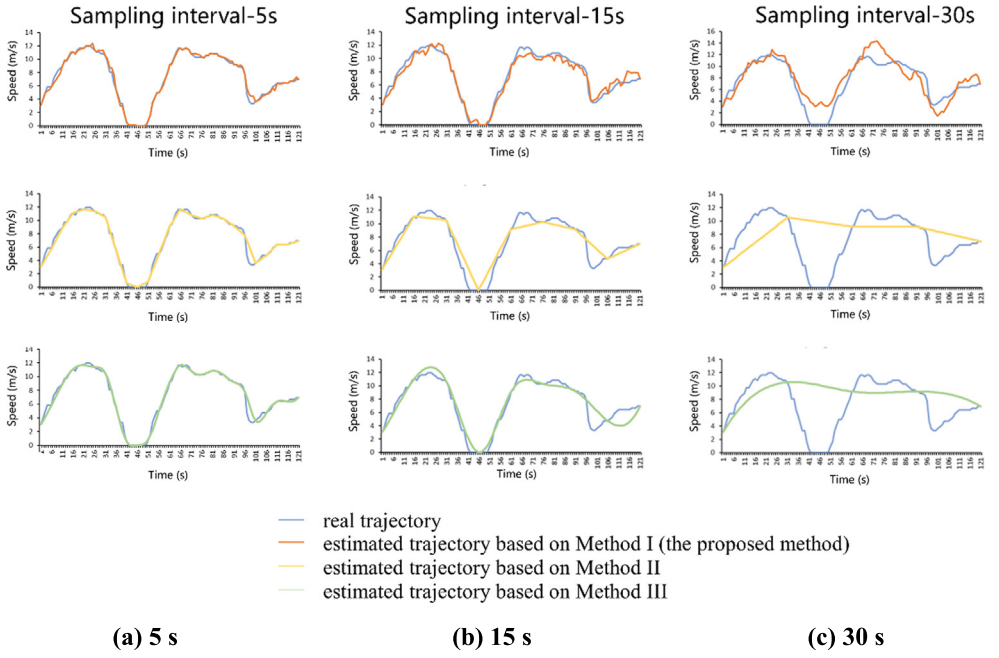

Fig. 3. Reconstructed trajectory results.

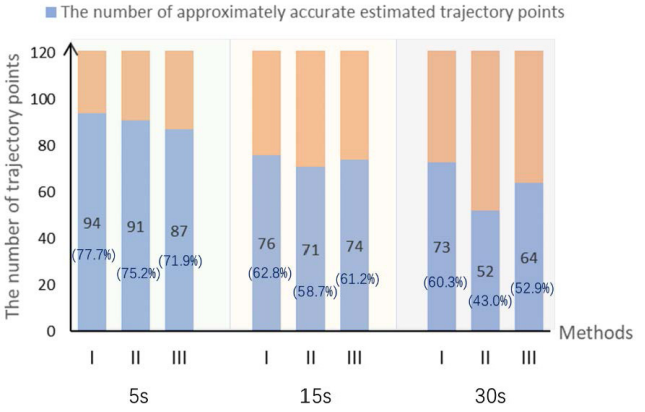

Fig. 4. The accuracy of trajectory reconstruction results.

4.2. Results of the SBS emission estimation model

A large number of fitting processes have been attempted based on different regression models, piecewise function establishment methods, and data binning methods. Representative and significant fitting results with good effects ($R^2 > 0.6$) are summarized according to the R^2 values, as presented in Table 2.

Compared with MOVES (the most widely used emission estimation model) and VT-Micro (the typical statistical regression model), the results of Model 6 proposed in this study showed the best performance ($R^2 = 0.887$). Model 1 was a polynomial regression model using discrete raw data after data cleaning, without establishing a piecewise function or dividing the data into bins ($R^2 = 0.695$). Model 2 was fitted with a piecewise function that included three states: deceleration, idling, and acceleration ($R^2 = 0.723$). Models 3 and 4 divided the data into several bins to reduce the number of raw data points. Model 3 was based on the curve estimation with VSP ($R^2 = 0.801$), and Model 4 was based on polynomial regression with speed, acceleration, and VSP ($R^2 = 0.831$). Models 2, 3, and 4 show some improvement in the goodness-of-fit compared to Model 1, which reflects the necessity of piecewise function and data binning. Therefore, both Models 5 and 6 were operated accordingly, and the former's piecewise function included only two states, i.e., deceleration and acceleration, similar to the VT-Micro model. Model 6 was divided the most, i.e., into three states, and the results showed that it had the best fit. Further

Table 2
Regression results table.

Model	Piecewise function	Binning	Regression result	R^2
1	No	No	$\ln ER = \beta_0 + \beta_1 v + \beta_2 va^2 + \beta_3 a^2 + \beta_4 VSP + \beta_5 v \cdot VSP + \beta_6 VSP^3$	0.695
2	Yes (III[#])	No	$\ln ER = \begin{cases} \beta_0^{dec} + \beta_1^{dec} v^2 + \beta_2^{dec} a^2 + \beta_3^{dec} VSP + \beta_4^{dec} v \cdot VSP + \beta_5^{dec} v, & deceleration \\ \beta_0^{acc} + \beta_1^{acc} VSP + \beta_2^{acc} v \cdot a \cdot VSP + \beta_3^{acc} v \cdot a + \beta_4^{acc} v^3 \cdot a^3, & acceleration \end{cases}$	0.723
3	No	Yes	$\ln ER = \beta_0 + \beta_1 VSP + \beta_2 VSP^2 + \beta_3 VSP^3$	0.801
4	No	Yes	$\ln ER = \beta_0 + \beta_1 VSP + \beta_2 v + \beta_3 VSP^3 + \beta_4 va^2 + \beta_5 a$	0.831
5	Yes (II[*])	Yes	$\ln ER = \begin{cases} \beta_0^{dec} + \beta_1^{dec} v^2 + \beta_2^{dec} VSP + \beta_3^{dec} v \cdot VSP, & deceleration \\ \beta_0^{acc} + \beta_1^{acc} VSP + \beta_2^{acc} VSP^2 + \beta_3^{acc} v + \beta_4^{acc} v^3, & acceleration \end{cases}$	0.864
6	Yes (III[#])	Yes	[**] $\ln ER = \begin{cases} \beta_0^{idling}, & idling \\ \beta_0^{dec} + \beta_1^{dec} v^2 + \beta_2^{dec} a^2 + \beta_3^{dec} VSP + \beta_4^{dec} v^2 \cdot a^2 + \beta_5^{dec} v \cdot VSP + \beta_6^{dec} v, & deceleration \\ \beta_0^{acc} + \beta_1^{acc} VSP + \beta_2^{acc} VSP^2 + \beta_3^{acc} v^3 + \beta_4^{acc} v + \beta_5^{acc} v^3 \cdot a^3 + \beta_6^{acc} v \cdot a^2 + \beta_7^{acc} a, & acceleration \end{cases}$	0.887
7	VT-Micro			0.845
8	MOVES			0.658

[*] II: states including deceleration and acceleration.
[#] III: states including idling, deceleration, and acceleration.
[**] the coefficients are: $\beta_0^{idling} =$ - 0.4987, $\beta_0^{dec} = -0.443$, $\beta_1^{dec} =$ 0.001, $\beta_2^{dec} =$ 0.011, $\beta_3^{dec} = 0.016$, $\beta_4^{dec} =$ 0.001, $\beta_5^{dec} = 0.001$, $\beta_6^{dec} =$ 0.013, $\beta_0^{acc} = 0.065$, $\beta_1^{acc} = 0.142$, $\beta_2^{acc} = -0.004$, $\beta_3^{acc} = 0.00003794$, $\beta_4^{acc} = -0.025$, $\beta_5^{acc} = 0.0000899$, $\beta_6^{acc} = -0.013$, $\beta_7^{acc} = 0.069$.

comparing other evaluation indexes of Model 6 and VT-Micro model, the mean absolute percentage errors (MAPEs) were 0.16 and 0.20, respectively. The root mean squared errors (RMSEs) were 0.38 and 0.41, respectively. These results demonstrated the significance of state subdivision and considering VSP to improve accuracy. Additionally, the comparison of the results between Model 5 and VT-Micro model, also directly demonstrated the necessity of VSP as an independent variable for emission estimation.

4.3. Emission estimation results based on sparse trajectory data

Using 30 real trajectory sequences of 120 s on arterials and collectors, the sampling intervals were 5, 15, and 30 s, respectively, and one trajectory sequence included several pieces with the corresponding sampling intervals. Trajectory reconstruction was conducted based on the interpolation method of acceleration distribution (Method I), linear interpolation (Method II), and cubic spline interpolation (Method III). Subsequently, carbon emissions were estimated by the SBS model using the reconstructed trajectories. The emission estimation comparison results are listed in Table 3.

The results presented in Table 3 indicate that the estimation of the method based on interpolation of acceleration distribution is better than that of the other two methods for all three sampling intervals. The results of 30 reconstructed trajectory sequences of 120 s show that the MAPEs of the total emission estimation of the sequences of Method I were 0.23, 1.07, and 1.52%, respectively, which were significantly lower than those of Methods II and III. As expected, the underestimation of emissions of the other two methods was significant, because the reconstructed trajectories were relatively stable. Notably, the sparser the sampling interval, the more the simple interpolation methods underestimated the emission. Considering trajectory pieces of 5, 15, and 30 s, respectively, as the analysis objects, Method I also showed the best performance. The MAPEs of this method were 3.51, 3.60, and 4.45%, while those of the other two methods were 4.30, 5.03, and 11.25% at intervals of 5, 15, and 30 s. The method proposed in this study has strong robustness, according to the emission estimation results at different sampling frequencies.

Table 3
Emission estimation comparison results.

Sampling interval	5 s			15 s			30 s		
Method	I[*]	II	III	I[*]	II	III	I[*]	II	III
MAPE of sequences (%)	0.23	3.28	2.75	1.07	6.13	4.83	1.52	11.07	10.60
MAPE of pieces (%)	3.51	4.57	4.30	3.60	6.47	5.03	4.45	12.56	11.25

[*] The proposed method.

5. Conclusions

Sparse trajectory data are more common than SBS trajectory data. However, there is a contradiction between the SBS input requirements of most emission estimation models and the difficulty in acquiring SBS data. Additionally, the existing carbon emission estimation models for motor vehicles have various limitations regarding their practical applications. Some models ignore the emission generation principle, and some studies have complicated inputs. To address these limitations, this study proposed a vehicle carbon emission estimation method for urban traffic based on sparse trajectory data.

First, a reconstruction method for sparse trajectory data based on interpolation of acceleration distribution was proposed. The estimated SBS trajectory data are the foundation of emission estimation. The results showed that the trajectory reconstructed by the method proposed in this study can better reproduce the real trajectory at different sampling frequencies than other interpolation reconstruction methods. Second, a motor vehicle carbon emission estimation model based on SBS trajectory data was proposed. The inputs of the model are convenient for acquisition, and the emission generation principle is considered. The results showed that the model performed best (R^2 = 0.887) compared to other commonly used models.

The emission estimation results for the sparse trajectory data of the case study showed that the method proposed in this study can improve the emission estimation precision at both low and high sampling frequencies. Compared to those of other interpolation methods, the precision of the proposed method is approximately 9% higher for low-frequency data and 2% higher for high-frequency data. These results demonstrate that the proposed method is robust.

However, this study has some limitations. The research object of this study is individual vehicle in urban traffic flow; thus, further detailed analyses and demonstrations are required for expressways. Additionally, factors such as traffic volume and traffic mix are worth being explored on a more macroscopic level in future research. The sparse trajectories for reconstruction contain fixed sampling intervals in this study, whereas unstable uploading of trajectory data may result in unequal intervals in reality. Solving this problem will help expand the generalizability of this method.

CRediT authorship contribution statement

Wanjing Ma: Conceptualization, Supervision, Writing – review & editing. **Yuhan Liu:** Investigation, Methodology, Validation, Writing – original draft, Writing – review & editing. **Philip Kofi Alimo:** Writing – review & editing. **Ling Wang:** Conceptualization, Investigation, Methodology, Visualization, Writing – review & editing.

Declaration of competing interest

The authors declare that they have no known competing financial interests or personal relationships that could have appeared to influence the work reported in this paper.

Acknowledgements

This research is supported by the National Natural Science Foundation of China (No. 52131204, 52325210, and 52102415), the Fundamental Research Funds for the Central Universities (2023-4-YB-05).

References

Chang, X., Chen, B.Y., Li, Q., Cui, X., Tang, L., Liu, C., 2012. Estimating real-time traffic carbon dioxide emissions based on intelligent transportation system technologies. IEEE Trans. Intell. Transp. Syst. 14, 469–479. https://doi.org/10.1109/TITS.2012.2219529.
Chen, B., Ding, C., Ren, W., Xu, G., 2021. Automatically tracking road centerlines from low-frequency GPS trajectory data. ISPRS Int. J. Geo Inf. 10, 122. https://doi.org/10.3390/ijgi10030122.
Chen, X., Zhang, S., Li, L., Li, L., 2018. Adaptive rolling smoothing with heterogeneous data for traffic state estimation and prediction. IEEE Trans. Intell. Transp. Syst. 20, 1247–1258. https://doi.org/10.1109/TITS.2018.2847024.
Chen, X., Yin, J., Tang, K., Tian, Y., Sun, J., 2022. Vehicle trajectory reconstruction at signalized intersections under connected and automated vehicle environment. IEEE Trans. Intell. Transp. Syst. 23, 17986–18000. https://doi.org/10.1109/TITS.2022.3150577.
Chindamo, D., Gadola, M., 2018. What is the most representative standard driving cycle to estimate diesel emissions of a light commercial vehicle? IFAC-PapersOnLine 51, 73–78. https://doi.org/10.1016/j.ifacol.2018.06.213.
Davis, N., Lents, J., Osses, M., Nikkila, N., Barth, M., 2005. Development and application of an international vehicle emissions model. Transp. Res. Rec. 1939, 156–165. https://doi.org/10.1177/0361198105193900118.
di Battista, D., Cipollone, R., 2016. Experimental and numerical assessment of methods to reduce warm up time of engine lubricant oil. Appl. Energy 162, 570–580. https://doi.org/10.1016/j.apenergy.2015.10.127.
EMFAC, V. 2006. 2.30: Calculating Emission Inventories for Vehicles in California, User's Guide. CARB.
EPA, U. 2003. User's Guide to MOBILE6. 1 and MOBILE6. 2. Environmental Protection Agency.
Grote, M., Williams, I., Preston, J., Kemp, S., 2018. A practical model for predicting road traffic carbon dioxide emissions using Inductive Loop Detector data. Transp. Res. Part D: Transp. Environ. 63, 809–825. https://doi.org/10.1016/j.trd.2018.06.026.
Hao, P., Boriboonsomsin, K., Wu, G., Barth, M., 2014. Probabilistic model for estimating vehicle trajectories using sparse mobile sensor data. In: 17th International IEEE Conference on Intelligent Transportation Systems (ITSC). IEEE, pp. 1363-1368. https://doi.org/10.1109/ITSC.2014.6957877.
Hao, P., Wu, G., Boriboonsomsin, K., Barth, M., 2016. Modal activity-based vehicle energy/emissions estimation using sparse mobile sensor data. In: Transportation Research Board 95th Annual Meeting. https://doi.org/10.1109/TITS.2016.2584388.
Härdle, W.K., Simar, I., 2019. Applied multivariate statistical analysis. Springer Nature. https://doi.org/10.1007/978-3-030-26006-4.
He, L., Hu, J., Zhang, S., Wu, Y., Zhu, R., Zu, L., Bao, X., Lai, Y., Su, S., 2018. The impact from the direct injection and multi-port fuel injection technologies for gasoline vehicles on solid particle number and black carbon emissions. Appl. Energy 226, 819–826. https://doi.org/10.1016/j.apenergy.2018.06.050.

International Energy Agency, 2021. Global Energy Review: CO2 Emissions in 2021. [Online]. Available: https://www.iea.org/reports/global-energy-review-co2-emissions-in-2021-2 [Accessed 2023-01-05].
Jimenez-Palacios, J.L. 1998. Understanding and quantifying motor vehicle emissions with vehicle specific power and TILDAS remote sensing. Massachusetts Institute of Technology. http://cires1.colorado.edu/jimenez/Papers/Jimenez_PhD_Thesis.pdf.
Kan, Z., Tang, L., Kwan, M.-P., Zhang, X., 2018. Estimating vehicle fuel consumption and emissions using GPS big data. Int. J. Environ. Res. Public Health 15, 566. https://doi.org/10.3390/ijerph15040566.
Lejri, D., Can, A., Schiper, N., Leclercq, L., 2018. Accounting for traffic speed dynamics when calculating COPERT and PHEM pollutant emissions at the urban scale. Transp. Res. Part D: Transp. Environ. 63, 588–603. https://doi.org/10.1016/j.trd.2018.06.023.
Li, Z., Kluger, R., Hu, X., Wu, Y.-J., Zhu, X., 2018. Reconstructing vehicle trajectories to support travel time estimation. Transp. Res. Rec. 2672, 148–158. https://doi.org/10.1177/0361198118772956.
Li, Z., Song, G., Yu, X., Yu, L., He, W., 2019. Developing operating mode distributions from sparse trajectories for emission estimation. Transp. Res. Rec. 2673, 137–148. https://doi.org/10.1177/0361198118821926.
Liu, H., Chen, X., Wang, Y., Han, S., 2013. Vehicle emission and near-road air quality modeling for shanghai, china: Based on global positioning system data from taxis and revised moves emission inventory. Transp. Res. Rec. 2340, 38–48. https://doi.org/10.3141/2340-05.
Liu, J., Han, K., Chen, X.M., Ong, G.P., 2019. Spatial-temporal inference of urban traffic emissions based on taxi trajectories and multi-source urban data. Transp. Res. Part C: Emerg. Technol. 106, 145–165. https://doi.org/10.1016/j.trc.2019.07.005.
Liu, J., Li, J., Chen, Y., Lian, S., Zeng, J., Geng, M., Zheng, S., Dong, Y., He, Y., Huang, P., 2023. Multi-scale urban passenger transportation CO_2 emission calculation platform for smart mobility management. Appl. Energy 331,. https://doi.org/10.1016/j.apenergy.2022.120407 120407.
Ma, Y., Zhu, J., 2021. Left-turn conflict identification at signal intersections based on vehicle trajectory reconstruction under real-time communication conditions. Accid. Anal. Prev. 150,. https://doi.org/10.1016/j.aap.2020.105933 105933.
Mingolla, S., Lu, Z., 2021. Carbon emission and cost analysis of vehicle technologies for urban taxis. Transp. Res. Part D: Transp. Environ. 99,. https://doi.org/10.1016/j.trd.2021.102994 102994.
Nam, E.K., Giannelli, R., 2005. Fuel consumption modeling of conventional and advanced technology vehicles in the physical emission rate estimator (PERE). US environmental protection agency.
Ntziachristos, L., Gkatzoflias, D., Kouridis, C. & Samaras, Z., 2009. COPERT: a European road transport emission inventory model. In: Information technologies in environmental engineering. Springer. https://doi.org/10.1007/978-3-540-88351-7_37.
Pathak, S.K., Sood, V., Singh, Y., Channiwala, S., 2016. Real world vehicle emissions: their correlation with driving parameters. Transp. Res. Part D: Transp. Environ. 44, 157–176. https://doi.org/10.1016/j.trd.2016.02.001.
Qin, W., Zhang, M., Li, W., Liang, Y., 2023. Spatiotemporal K-nearest neighbors algorithm and Bayesian approach for estimating urban link travel time distribution from sparse GPS trajectories. IEEE Intell. Transp. Syst. Mag. https://doi.org/10.1109/MITS.2023.3296331.
Quddus, M., Washington, S., 2015. Shortest path and vehicle trajectory aided map-matching for low frequency GPS data. Transp. Res. Part C: Emerg. Technol. 55, 328–339. https://doi.org/10.1016/j.trc.2015.02.017.
Rakha, H., Ahn, K., Trani, A., 2004. Development of VT-Micro model for estimating hot stabilized light duty vehicle and truck emissions. Transp. Res. Part D: Transp. Environ. 9, 49–74. https://doi.org/10.1016/S1361-9209(03)00054-3.
Raymand, F., Ahmadi, P., Mashayekhi, S., 2021. Evaluating a light duty vehicle fleet against climate change mitigation targets under different scenarios up to 2050 on a national level. Energy Policy 149,. https://doi.org/10.1016/j.enpol.2020.111942 111942.
Scora, G., Barth, M., 2006. Comprehensive modal emission model (cmem) version 3.01 user's guide. University of California, Riverside, 7.
Shafabakhsh, G., Taghizadeh, S.A., Mehrabi Kooshki, S., 2018. Investigation and sensitivity analysis of air pollution caused by road transportation at signalized intersections using IVE model in Iran. Eur. Transp. Res. Rev. 10, 1–13. https://doi.org/10.1007/s12544-017-0275-3.
Shan, X., Hao, P., Chen, X., Boriboonsomsin, K., Wu, G., Barth, M.J., 2018. Vehicle energy/emissions estimation based on vehicle trajectory reconstruction using sparse mobile sensor data. IEEE Trans. Intell. Transp. Syst. 20, 716–726. https://doi.org/10.1109/TITS.2018.2826571.
Shang, W.-L., Zhang, M., Wu, G., Yang, L., Fang, S., Ochieng, W., 2023. Estimation of traffic energy consumption based on macro-micro modelling with sparse data from Connected and Automated Vehicles. Appl. Energy 351,. https://doi.org/10.1016/j.apenergy.2023.121916 121916.
Smit, R., Smokers, R., Rabé, E., 2007. A new modelling approach for road traffic emissions: VERSIT+. Transp. Res. Part D: Transp. Environ. 12, 414–422. https://doi.org/10.1016/j.trd.2007.05.001.
Song, G., Yu, L., 2009. Estimation of fuel efficiency of road traffic by characterization of vehicle-specific power and speed based on floating car data. Transp. Res. Rec. 2139, 11–20. https://doi.org/10.3141/2139-02.
Song, G., Yu, L., 2011. Characteristics of low-speed vehicle-specific power distributions on urban restricted-access roadways in beijing. Transp. Res. Rec. 2233, 90–98. https://doi.org/10.3141/2233-11.
Sun, Z., Hao, P., Ban, X.J., Yang, D., 2015. Trajectory-based vehicle energy/emissions estimation for signalized arterials using mobile sensing data. Transp. Res. Part D: Transp. Environ. 34, 27–40. https://doi.org/10.1016/j.trd.2014.10.005.
Sun, Y.-F., Zhang, Y.-J., Su, B., 2022. How does global transport sector improve the emissions reduction performance? A demand-side analysis. Appl. Energy 311,. https://doi.org/10.1016/j.apenergy.2022.118648 118648.
Turkensteen, M., 2017. The accuracy of carbon emission and fuel consumption computations in green vehicle routing. Eur. J. Oper. Res. 262, 647–659. https://doi.org/10.1016/j.ejor.2017.04.005.
U.S. Environmental Protection Agency, 2021. Overview of EPA's MOtor Vehicle Emission Simulator (MOVES3). [Online]. Available: https://nepis.epa.gov/Exe/ZyPDF.cgi?Dockey=P1011KV2.pdf [Accessed 2023-01-05].
Venthuruthiyil, S.P., Chunchu, M., 2018. Trajectory reconstruction using locally weighted regression: a new methodology to identify the optimum window size and polynomial order. Transportmetrica A: Transport Sci. 14, 881–900. https://doi.org/10.1080/23249935.2018.1449032.
Wang, S., Li, Z., Tan, J., Guo, W., Li, L., 2017. A method for estimating carbon dioxide emissions based on low frequency GPS trajectories. In: 2017 Chinese Automation Congress (CAC), 2017. IEEE, pp. 1960–1964. https://doi.org/10.1109/CAC.2017.8243091.
Wang, H., Gu, C., Ochieng, W.Y., 2019. Vehicle trajectory reconstruction for signalized intersections with low-frequency floating car data. J. Adv. Transp. 2019, 1–14. https://doi.org/10.1155/2019/9417471.
Weng, J., Liang, Q., Qiao, G., Chen, Z., Rong, J., 2017. Taxi fuel consumption and emissions estimation model based on the reconstruction of driving trajectory. Adv. Mech. Eng. 9,. https://doi.org/10.1177/1687814017708708 1687814017708708.
Xie, X., van Lint, H., Verbraeck, A., 2018. A generic data assimilation framework for vehicle trajectory reconstruction on signalized urban arterials using particle filters. Transp. Res. Part C: Emerg. Technol. 92, 364–391. https://doi.org/10.1016/j.trc.2018.05.009.
Xu, J., Hilker, N., Turchet, M., Al-Rijleh, M.-K., Tu, R., Wang, A., Fallahshorshani, M., Evans, G., Hatzopoulou, M., 2018. Contrasting the direct use of data from traffic radars and video-cameras with traffic simulation in the estimation of road emissions and PM hotspot analysis. Transp. Res. Part D: Transp. Environ. 62, 90–101. https://doi.org/10.1016/j.trd.2018.02.010.
Yang, Q., Boriboonsomsin, K., Barth, M., 2011. Arterial roadway energy/emissions estimation using modal-based trajectory reconstruction. In: 2011 14th International IEEE Conference on Intelligent Transportation Systems (ITSC). IEEE, pp. 809–814. https://doi.org/10.1109/ITSC.2011.6083069.
Zhang, Y., Ioannou, P.A., 2016. Environmental impact of combined variable speed limit and lane change control: a comparison of MOVES and CMEM model. IFAC-PapersOnLine 49, 323–328. https://doi.org/10.1016/j.ifacol.2016.07.054.
Zhang, Z., Song, G., Zhai, Z., Li, C., Wu, Y., 2019. How many trajectories are needed to develop facility-and speed-specific vehicle-specific power distributions for emission estimation? Case study in Beijing. Transp. Res. Rec. 2673, 779–790. https://doi.org/10.1177/0361198119853550.
Zhao, B., Lin, Y., Hao, H., Yao, Z., 2022. Fuel consumption and traffic emissions evaluation of mixed traffic flow with connected automated vehicles at multiple traffic scenarios. J. Adv. Transp. 2022, 1–14. https://doi.org/10.1155/2022/6345404.